Proxy Synthesis: Learning with Synthetic Classes for Deep Metric Learning

Geonmo Gu[*1], **Byungsoo Ko**[*1], **Han-Gyu Kim** [2]
[1] NAVER/LINE Vision, [2] NAVER Clova Speech
korgm403@gmail.com, kobiso62@gmail.com, hangyu.kim@navercorp.com

Abstract

One of the main purposes of deep metric learning is to construct an embedding space that has well-generalized embeddings on both *seen* (training) classes and *unseen* (test) classes. Most existing works have tried to achieve this using different types of metric objectives and hard sample mining strategies with given training data. However, learning with only the training data can be overfitted to the *seen* classes, leading to the lack of generalization capability on *unseen* classes. To address this problem, we propose a simple regularizer called *Proxy Synthesis* that exploits synthetic classes for stronger generalization in deep metric learning. The proposed method generates synthetic embeddings and proxies that work as synthetic classes, and they mimic *unseen* classes when computing proxy-based losses. *Proxy Synthesis* derives an embedding space considering class relations and smooth decision boundaries for robustness on *unseen* classes. Our method is applicable to any proxy-based losses, including softmax and its variants. Extensive experiments on four famous benchmarks in image retrieval tasks demonstrate that *Proxy Synthesis* significantly boosts the performance of proxy-based losses and achieves state-of-the-art performance. Our implementation is available at *github.com/navervision/proxy-synthesis*.

1 Introduction

Deep metric learning aims to learn a similarity metric among arbitrary data points so that it defines an embedding space where semantically similar images are close together, and dissimilar images are far apart. Owing to its practical significance, it has been used for a variety of tasks such as image retrieval (Gordo et al. 2016; Sohn 2016), person re-identification (Yu et al. 2018; Hermans, Beyer, and Leibe 2017), zero-shot learning (Zhang and Saligrama 2016), and face recognition (Wen et al. 2016; Deng et al. 2019). The well-structured embedding is requested to distinguish the *unseen* classes properly, where the model is required to learn image representation from *seen* classes. This has been achieved by loss functions, which can be categorized into two types: *pair-based* and *proxy-based* loss.

The pair-based losses are designed based on the pairwise similarity between data points in the embedding space, such as contrastive (Chopra, Hadsell, and LeCun 2005), triplet (Weinberger and Saul 2009), N-pair loss (Sohn 2016), *etc*. However, they require high training complexity and empirically suffer from sampling issues (Movshovitz-Attias et al. 2017). To address these issues, the concept of proxy has been introduced. A proxy is a representative of each class, which can be trained as a part of the network parameters. Given a selected data point as an anchor, proxy-based losses consider its relations with proxies. This alleviates the training complexity and sampling issues because only data-to-proxy relations are considered with a relatively small number of proxies compared to that of data points.

Although the performance of metric learning losses has been improved, a network trained only with training (*seen*) data can be overfitted to the *seen* classes and suffer from low generalization on *unseen* classes. To resolve this problem, previous works (Zheng et al. 2019; Gu and Ko 2020; Ko and Gu 2020) have generated synthetic samples to exploit additional training signals and more informative representations. However, these methods can only be used for pair-based losses; thus, they still suffer from the training complexity and sampling issues.

In this paper, we propose ***Proxy Synthesis*** (*PS*), which is a simple regularizer for proxy-based losses that encourages networks to construct better generalized embedding space for *unseen* classes. As illustrated in Figure 1, our method generates synthetic embeddings and proxies as synthetic classes for computing a proxy-based loss. *Proxy Synthesis* exploits synthetic classes generated by semantic interpolations to mimic *unseen* classes, obtaining smooth decision boundaries and an embedding space considering class relations. Moreover, the proposed method can be used with any proxy-based loss, including softmax loss and its variants. We demonstrate that our proposed method yields better robustness on *unseen* classes and deformation on the input and embedding feature. We achieve a significant performance boost on every proxy-based loss with *Proxy Synthesis* and obtain state-of-the-art performance with respect to four famous benchmarks in image retrieval tasks.

2 Related Work

Sample Generation: To achieve better generalization, previous works (Zhao et al. 2018; Duan et al. 2018; Zheng et al. 2019) have leveraged a generative network to cre-

[*]Authors contributed equally.

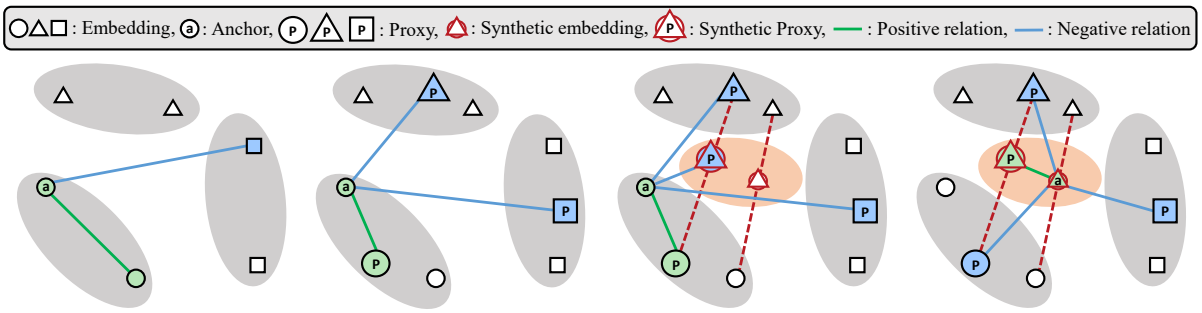

(a) Pair-based loss (b) Proxy-based loss (c) *Proxy Synthesis* + proxy-based loss

Figure 1: Comparison among concepts. (a) Pair-based loss maximizes similarity of positive pairs and minimizes similarity of negative pairs (i.e., Triplet loss). (b) Given an anchor embedding, proxy-based loss maximizes similarity with positive proxy and minimizes similarity with all negative proxies (i.e., Proxy NCA and Softmax variants). (c) *Proxy Synthesis* exploits synthetic classes in-between original classes for additional training signals and competitive hard classes.

ate synthetic samples, which can lead to a bigger model and slower training speed. To solve these problems, recent works (Gu and Ko 2020; Ko and Gu 2020) have proposed to generate samples by algebraic computation in the embedding space. However, the above works can only be used for pair-based losses, which causes the same drawbacks of high training complexity and careful pair mining. In addition, the above works exploit synthetic embeddings only for existing (*seen*) classes, when *Proxy Synthesis* uses synthetic embeddings and proxies as virtual classes for generalization on *unseen* classes explicitly.

Mixup: Mixup techniques (Zhang et al. 2017; Verma et al. 2018; Guo, Mao, and Zhang 2019) have been proposed for generalization in the classification task. These techniques linearly interpolate a random pair of training samples and the corresponding one-hot labels. *Proxy Synthesis* and Mixup techniques share the common concept in terms of interpolating features for augmentation but have three major differences. First, Mixup techniques are proposed for generalization, which aims for robustness on *seen* classes, such as classification, whereas *Proxy Synthesis* is proposed for generalization in metric learning tasks, aiming for robustness on *unseen* classes. Second, Mixup techniques interpolate the input vectors and hidden representations, whereas the proposed method interpolates the embedding features in the output space. Third, Mixup techniques interpolate one-hot labels, while *Proxy Synthesis* interpolates proxies, which allow us to learn the positional relations of class representatives in the embedding space explicitly.

Virtual Class: Virtual softmax (Chen, Deng, and Shen 2018) generates a single weight as a virtual negative class for softmax function to enhance the discriminative property of learned features in the classification task. Even though the work proves that the constrained region for each class becomes more compact by the number of classes increase, Virtual softmax considers a single synthetic weight without any corresponding embedding as a virtual negative class. Moreover, generating virtual weight by $W_{virt} = \|W_{y_i}\|x_i/\|x_i\|$ is not applicable for softmax variants with weight normalization (i.e. Norm-Softmax, ArcFace, Proxy-anchor, *etc*), where x_i is i-th embedding, and W_{y_i} is its positive class weight. This is because W_{virt} of the synthetic negative class will be equivalent to x_i after normalization. In contrast, *Proxy Synthesis* generates multiple proxies (weights) and corresponding embeddings as multiple virtual classes, which can be used as negative and also positive classes. Moreover, the proposed method is applicable for any proxy-based loss and softmax variants.

3 Proposed Method

3.1 Preliminary

Consider a deep neural network $f : \mathcal{D} \xrightarrow{f} \mathcal{X}$, which maps from an input data space $\mathcal{D}$ to an embedding space $\mathcal{X}$. We define a set of embedding feature $X = [x_1, x_2, \ldots, x_N]$, where each feature x_i has label of $y_i \in \{1, \ldots, C\}$ and N is the number of embedding features. We denote a set of proxy $P = [p_1, p_2, \ldots, p_C]$ and formulate generalized proxy-based loss as:

$$\mathcal{L}(X, P) = \mathop{\mathbb{E}}_{(x,p)\sim R} \ell(x, p), \tag{1}$$

where (x, p) denotes random pair of embedding and matching proxy from the pair distribution R.

Softmax loss is not only the most widely used classification loss but also has been re-valued as competitive loss in metric learning (Zhai and Wu 2018; Boudiaf et al. 2020). Let $W_j \in \mathbb{R}^d$ denote the j-th column of the weight $W \in \mathbb{R}^{d\times C}$, where d is the size of embedding features. Then, Softmax loss is presented as follows:

$$\mathcal{L}_{Softmax}(X) = -\frac{1}{|X|}\sum_{i=1}^{|X|} \log \frac{e^{W_{y_i}^T x_i}}{\sum_{j=1}^{C} e^{W_j^T x_i}}, \tag{2}$$

where we set the bias $b = 0$ because it does not affect the performance (Liu et al. 2017; Deng et al. 2019). Because the proxy P is learned as model parameter, the weight W of

softmax loss can be interpreted as proxy, which is the center of each class (Deng et al. 2019; Wang et al. 2018b).

Normalizing the weights and feature vector is proposed to lay them on a hypersphere of a fixed radius for better interpretation and performance (Wang et al. 2017, 2018a; Liu et al. 2017). When we transform the logit (Pereyra et al. 2017) as $W_j^T x_i = \parallel W_j \parallel \parallel x_i \parallel \cos\theta_j$ and fix the individual proxy (weight) $\parallel W_j \parallel = 1$ and feature $\parallel x_i \parallel = 1$ by l_2-normalization, the normalized softmax (Norm-softmax) loss can be written with proxy-wise form as:

$$\mathcal{L}_{Norm}(X,P) = -\frac{1}{|X|}\sum_{x\in X}\log\frac{e^{\gamma s(x,p^+)}}{e^{\gamma s(x,p^+)}+\sum\limits_{q\in P^-}e^{\gamma s(x,q)}}, \quad (3)$$

where p^+ is a positive proxy, P^- is a set of negative proxies, γ is a scale factor, and $s(a,b)$ denotes the cosine similarity between a and b. More details of proxy-based (Proxy-NCA (Movshovitz-Attias et al. 2017), SoftTriple (Qian et al. 2019), and Proxy-anchor (Kim et al. 2020)) and softmax variants (SphereFace (Liu et al. 2017), ArcFace (Deng et al. 2019), and CosFace (Wang et al. 2018b)) losses are presented in the supplementary Section A.

3.2 Proxy Synthesis

One of the key purposes of metric learning is to construct a robust embedding space for *unseen* classes. For this purpose, the proposed method allows proxy-based losses to exploit synthetic classes. Training a proxy-based loss using *Proxy Synthesis* is performed in three steps. First, we process a mini-batch of input data with a network f to obtain a set of embeddings X. Second, given two random pairs of an embedding and corresponding proxy from different classes, (x,p) and (x',p'), we generate a pair of synthetic embedding and proxy $(\tilde{x},\tilde{p})$ as follows:

$$(\tilde{x},\tilde{p}) \equiv (I_\lambda(x,x'), I_\lambda(p,p')), \quad (4)$$

where $I_\lambda(a,b) = \lambda a + (1-\lambda)b$ is a linear interpolation function with the coefficient of $\lambda \sim Beta(\alpha,\alpha)$ for $\alpha \in (0,\infty)$, and $\lambda \in [0,1]$. We perform $\mu \times batch\,size$ generations of Eq. 4, where hyper-parameter $\mu = \frac{\#\,of\,synthetics}{batch\,size}$ is a generation ratio by batch size. Thereafter, we define $\widehat{X}$ as a set of original and synthetic embeddings, and $\widehat{P}$ as a set of original and synthetic proxies. Synthetic proxy $\tilde{p}$ will work as a representative of the synthetic class, which has a mixed representation of class p and p', whereas the synthetic embedding $\tilde{x}$ will be a synthetic data point of the synthetic class. Third, we compute the loss, including synthetic embeddings and proxies, as if they are new classes. The generalized loss with *Proxy Synthesis* is formulated as:

$$\mathcal{L}(\widehat{X},\widehat{P}) = \mathop{\mathbb{E}}_{\lambda\sim Beta(\alpha,\alpha)}\ \mathop{\mathbb{E}}_{(x,p)\sim\widehat{R_\lambda}}\ \ell(x,p), \quad (5)$$

where $\widehat{R_\lambda}$ is a distribution of the embedding and proxy pairs including originals and synthetics generated with λ. Implementing *Proxy Synthesis* is extremely simple with few lines of codes. Moreover, it does not require to modify any code of proxy-based loss and can be used in a plug-and-play manner with negligible computation cost. Code-level description and experiment of training time and memory are presented in the supplementary Section B.1 and D.1, respectively.

3.3 Discussion

Learning with Class Relations: Unlike tasks that only test with *seen* classes such as classification, metric learning is desired to construct a structural embedding space for robustness on *unseen* classes. A well-structured embedding space should contain meaningful relations among embeddings; an example from the previous work (Mikolov et al. 2013) is as follows: $king - man + woman \approx queen$ in a word embedding space. To achieve this, *Proxy Synthesis* explicitly inserts in-between class relations with synthetic classes (i.e., $I_\lambda(wolf, dog) \approx wolfdog$) and they mimic unseen classes for training with a diverse range of data characteristics. *Proxy Synthesis* considers class relations with Equation 4 and 5 in forward propagation. This characteristic is reflected in backward propagation as well.

For convenience in gradient analysis, we write the loss of softmax function on (x,p_i), where x is an anchor embedding of input, and p_i is corresponding positive proxy, as follows,

$$\mathcal{L}_i = \mathcal{L}_{Softmax}(x,p_i) = -\log\frac{E(p_i)}{E(p_i)+\sum_{q\in P^-}E(q)}, \quad (6)$$

where $E(p) = e^{S(x,p)}$ and $S(x,p) = s(x,p) \parallel x \parallel \parallel p \parallel = x^T p$. Then, gradient over positive similarity $S(x,p_i)$ is,

$$\frac{\partial\mathcal{L}_i}{\partial S(x,p_i)} = \frac{E(p_i)}{\sum_{q\in P}E(q)} - 1. \quad (7)$$

It shows that the gradient over $S(x,p_i)$ only considers the similarity of the anchor embedding and its proxy by $E(p_i)$.

When *Proxy Synthesis* is applied, the gradient changes. In this gradient induction, we assume that the positive proxy p_i of input is used for generating synthesized proxy $\tilde{p}$ with p_j as $\tilde{p} = \lambda p_i + \lambda' p_j$, where $\lambda' = 1-\lambda$. Then, the gradients over $S(x,p_i)$ and $S(x,p_j)$ are inducted as follows,

$$\frac{\partial\mathcal{L}_i}{\partial S(x,p_i)} = \frac{\lambda E(\tilde{p})+E(p_i)}{E(\tilde{p})+\sum_{q\in P}E(q)} - 1, \quad (8)$$

$$\frac{\partial\mathcal{L}_i}{\partial S(x,p_j)} = \frac{\lambda' E(\tilde{p})+E(p_j)}{E(\tilde{p})+\sum_{q\in P}E(q)}. \quad (9)$$

In contrast to the softmax loss, *Proxy Synthesis* enables the gradient over $S(x,p_i)$ and $S(x,p_j)$ to consider class relation between p_i and p_j via $E(\tilde{p}) = E(\lambda p_i + \lambda' p_j)$ in the backward propagation. The detailed induction is presented in supplementary Section B.2.

Obtaining a Smooth Decision Boundary: Synthetic classes work as hard competitors of original classes because of positional proximity, which leads to lower prediction confidence and, thus, smoother decision boundaries. The smoothness of the decision boundary is a main factor of generalization (Bartlett and Shawe-Taylor 1999; Verma et al. 2018), and it is more desirable in metric learning to provide a relaxed estimate of uncertainty for *unseen* classes. For better intuitions, we conduct an experiment to visualize the generalization effect of *Proxy Synthesis*, as depicted in Figure 2. For both the input and embedding spaces, Norm-softmax has a strict decision boundary, whereas *PS* + Norm-softmax has a smooth decision boundary that transitions linearly from

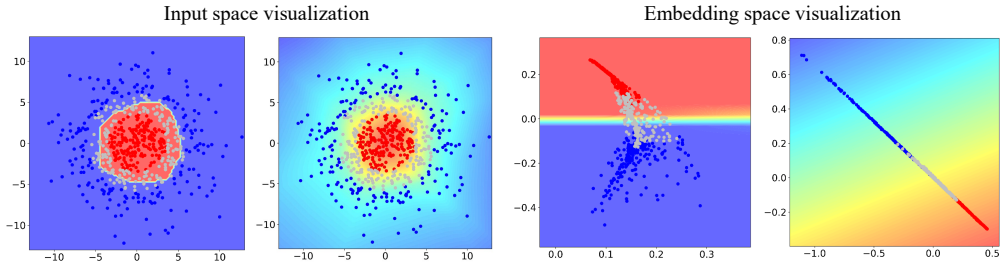

(a) Norm-softmax (b) *PS* + Norm-softmax (c) Norm-softmax (d) *PS* + Norm-softmax

Figure 2: Experiment with 2D isotropic Gaussian dataset including red, blue, and gray classes. Simple feed-forward network with two-dimensional embedding is used, while we train network with red and blue classes and let gray class remain *unseen*. The darker the intensity of the blue or red in the background, the higher the prediction confidence to blue or red class, respectively.

the red to the blue class. Further theoretical analysis of such phenomenon is provided below.

A network with ordinary softmax outputs the probability of an embedding x belonging to a specific class i as follows,

$$\texttt{Pr}(x,i) = \frac{e^{S(x,p_i)}}{e^{S(x,p_i)} + \sum_{q\in P\setminus\{p_i\}} e^{S(x,q)}}. \tag{10}$$

Considering the linearity of similarity function $S(x,p) = x^T p$, the strict decision boundary is constructed when the network always outputs embedding vector close to one proxy, even though the input has shared visual semantics among different classes. Such phenomenon occurs because the softmax function forces all embedding vectors to become as close to the corresponding proxies as possible during training. Considering the softmax loss of an embedding vector and its positive proxy (x,p_i) as Equation 6, the gradient of such loss over x can be inducted as follows:

$$\frac{\partial \mathcal{L}_i}{\partial x} = \tau_i p_i \quad + \sum_{p_k\in P^-} \tau_k p_k, \tag{11}$$

$$\tau_i = \frac{E(p_i)}{\sum_{q\in P} E(q)} - 1 \quad , \quad \tau_k = \frac{E(p_k)}{\sum_{q\in P} E(q)}. \tag{12}$$

It is obvious that $\tau_i < 0$ and $\tau_k > 0$. Considering the parameter update is performed by $x = x - \eta\frac{\partial \mathcal{L}_i}{\partial x}$, where η is a learning rate, the gradient descent forces x to be closer to p_i and to be distant from other proxies p_k.

Proxy Synthesis overcomes such problem of embedding space to overfit to the proxies by providing a gradient of opposite direction compared to ordinary softmax. To describe major difference of *Proxy Synthesis* and ordinary softmax, we consider softmax loss for synthesized pair $\tilde{x} = \lambda x + \lambda' x', \tilde{p} = \lambda p_i + \lambda' p_j$, where (x,p_i) and (x',p_j) are pairs of an embedding and a corresponding proxy:

$$\begin{aligned}\tilde{\mathcal{L}} &= \mathcal{L}_{Softmax}(\tilde{x},\tilde{p}) \\ &= -\log \frac{E(\tilde{p})}{E(\tilde{p}) + E(p_i) + E(p_j) + \sum_{q\in P^-} E(q)},\end{aligned} \tag{13}$$

where $E(p) = e^{S(\tilde{x},p)}$ and $P^- = P \setminus \{p_i, p_j\}$. It should be noted that $\tilde{p} \notin P$. Since we suggest to sample λ from $Beta(\alpha,\alpha)$ with small α in Section 4.3, $\tilde{p}$ has high chance to be generated either close to p_i with $\lambda >> 0.5$ or close to p_j with $\lambda << 0.5$. As the proofs for both cases are equivalent, we assume the first case: $\tilde{x}$ is much closer to x than x'. We consider gradient over x because the loss will affect the closer embedding vector more than the other one. The inducted gradient over x is as follows:

$$\frac{\partial \tilde{\mathcal{L}}}{\partial x} = -\lambda \frac{\sum_{q\in P}(\tilde{p}-q)E(q)}{E(\tilde{p}) + \sum_{q\in P} E(q)}. \tag{14}$$

As $\tilde{x}$ is closer to p_i and $\tilde{p}$ compared to other proxies, $E(p_i), E(\tilde{p}) >> E(q) \quad \forall q \neq p_i, \tilde{p}$. Thus, Equation 14 can be re-written as follows,

$$\frac{\partial \tilde{\mathcal{L}}}{\partial x} \approx -\lambda \frac{(\tilde{p}-p_i)E(p_i)}{E(\tilde{p}) + E(p_i)} = \tau_i' p_i + \tau_j' p_j, \tag{15}$$

$$\tau_i' = \frac{\lambda\lambda' E(p_i)}{E(\tilde{p}) + E(p_i)}, \quad \tau_j' = -\frac{\lambda\lambda' E(p_i)}{E(\tilde{p}) + E(p_i)}. \tag{16}$$

It is obvious that $\tau_i' > 0$, implying that by adopting *Proxy Synthesis*, softmax loss for synthesized pair provides gradient which leads embedding vector not too close to the corresponding proxy p_i; it is also obvious that $\tau_j' < 0$, implying that softmax loss for synthesized pair provides gradient which makes embedding vector not too distant from the competing proxy p_j. In such a manner, *Proxy Synthesis* prevents embedding vectors lying too close to proxies, which finally leads to the smooth decision boundary. The detailed induction is provided in the supplementary Section B.3.

4 Experiments

4.1 Experimental Setting

We evaluate the proposed method with respect to four benchmarks in metric learning: CUB-200-2011 (CUB200) (Wah et al. 2011), CARS196 (Krause et al. 2013), Standford Online Products (SOP) (Oh Song et al. 2016), and In-Shop Clothes (In-Shop) (Liu et al. 2016). We follow the widely used training and evaluation procedure from (Oh Song et al. 2016; Kim et al. 2020) and call it *conventional evaluation*. Experiments are performed on an Inception network with batch normalization (Ioffe and Szegedy 2015) with a 512 embedding dimension. For the hyper-parameters of *Proxy Synthesis*, α and μ are set to

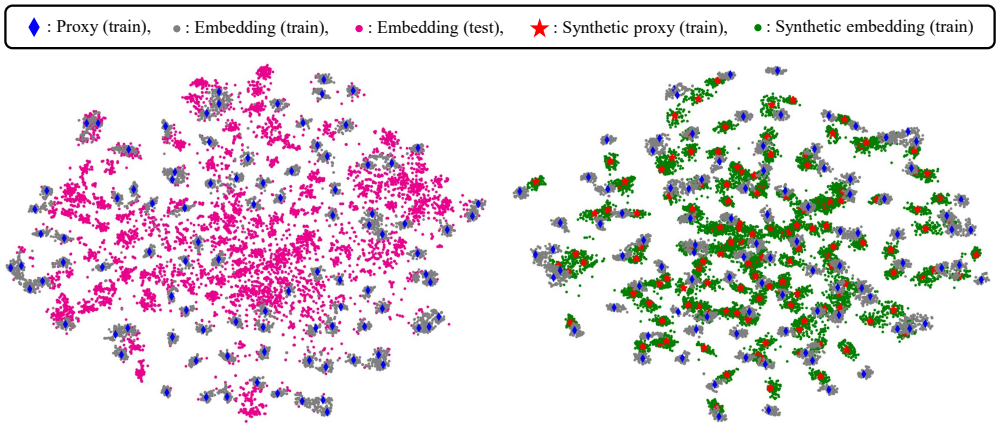

(a) Original train + original test (b) Original train + synthetic train

Figure 3: t-SNE visualization (Maaten and Hinton 2008) of converged network trained with *PS* + Norm-softmax loss on CARS196. (a) We project both train (*seen*) and test (*unseen*) embeddings. (b) With the same train embeddings as in (a), we project synthetic embeddings and proxies.

Model	Embedding		Proxy		R@1
	Original	Synthetic	Original	Synthetic	
M1 (baseline)	✓		✓		83.3
M2		✓		✓	83.1
M3	✓		✓	✓	83.7
M4		✓	✓	✓	83.7
Proxy Synthesis	✓	✓	✓	✓	**84.7**

Table 1: Recall@1(%) comparison among different usages of original and synthetic embedding and proxy on CARS196. We set elements of $\widehat{X}$ and $\widehat{P}$ to be checked(✓) embeddings and proxies to compute $\mathcal{L}_{Norm}(\widehat{X}, \widehat{P})$.

λ	R@1(%)
0.1	83.1
0.2	**83.8**
0.3	83.7
0.4	83.5
0.5	83.3

(a) Static generation

α	R@1(%)
0.2	84.0
0.4	**84.7**
0.8	83.9
1.0	83.7
1.5	83.7

(b) Stochastic generation

Table 2: Comparison between static and stochastic generation of synthetics while training with *PS* + Norm-softmax on CARS196. For static generation, synthetics are generated with fixed value of λ. For stochastic generation, synthetics are generated with sampled λ from $Beta(\alpha, \alpha)$.

0.4 and 1.0, respectively. Considering recent works (Musgrave, Belongie, and Lim 2020; Fehervari, Ravichandran, and Appalaraju 2019) that have presented enhanced evaluation procedure with regard to fairness, we include an evaluation procedure designed from work "A metric learning reality check" (Musgrave, Belongie, and Lim 2020) and call it *MLRC evaluation*, which contains 4-fold cross-validation, ensemble evaluation, and usage of fair metrics (P@1, RP, and MAP@R). Please refer to supplementary Section C for further details on the benchmarks and implementation.

4.2 Impact of Synthetic Class

Embedding Space Visualization: Exploiting synthetic classes is preferable in metric learning because the main goal is to develop robustness on *unseen* classes. This is depicted visually in Figure 3. In Figure 3a, *unseen* test embeddings are located in-between the clusters of train embeddings by forming clusters. Similarly, synthetic classes are also generated in-between train embeddings, as depicted in Figure 3b, and play an important role in mimicking *unseen* classes during the training phase. Thus, these additional training signals enable a network to capture extra discriminative features for better robustness on *unseen* classes. Extended visualization is in supplementary Section D.5.

Impact of Synthetic Embedding and Proxy: To investigate the quantitative impact of synthetic embedding and proxy, we conduct an experiment by differentiating the elements of $\widehat{X}$ and $\widehat{P}$ in Norm-softmax loss. Table 1 illustrates that using only synthetic embeddings and proxies (M2) leads to a slightly lower performance than the baseline (M1). Adding synthetic proxies (M3) and using synthetic embedding instead of the original embedding (M4) leads to improved performance when compared with the baseline (M1). This indicates that the generated synthetic embeddings and proxies build meaningful virtual classes for training. Finally, using all embeddings and proxies (*Proxy Synthesis*) achieves the best performance among all cases by considering the fundamental and additional training signals.

4.3 Synthetic Class as Hard Competitor

Impact of Hardness: Generating synthetic classes is required to be hard enough so that the model can learn more discriminative representations. The hardness of synthetic classes can be controlled by α, which decides probability distribution for the sampling of the interpolation coefficient

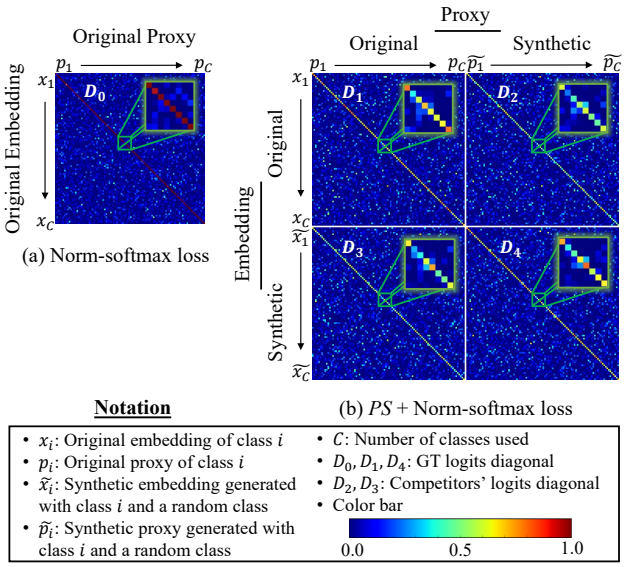

Figure 4: Heatmap visualization of cosine similarity (logit) at 100th epoch of training on CARS196. (a) Norm-softmax loss with original embedding and proxy. (b) *PS* + Norm-softmax loss including synthetic embedding and proxy.

λ. In Table 2, static $\lambda = 0.1$ shows low performance because synthetic classes are too close to original classes, and static $\lambda = 0.5$ also shows low performance because it generates synthetic classes in the middle of two original classes, which is relatively easy to distinguish. The optimal static λ value is around 0.2, which establishes the proper difficulty of distinguishment. Moreover, the result shows that the stochastic generation is better than the static generation. This is because stochastic generation can generate more number of different synthetic classes with wide variation. In the stochastic generation, $\alpha = 1.0$ is the same with uniform distribution, and $\alpha = 1.5$ has a high chance of generating synthetics in the middle of two classes; thus, their performance is relatively low. Similar to the experiment of static generation, α around 0.4 shows the best performance, which has a high chance of generating synthetic classes close enough to an original class. We provide additional experiments on the effect of hyper-parameter in supplementary Section D.2.

Logits Visualization: We compare the cosine similarity (logits) between embeddings and proxies during the training procedure. In Figure 4a, the logit values of ground truth (GT), which are represented by the main diagonal D_0, are clearly red owing to high prediction confidence. This leads to a strict decision boundary, as depicted in Figure 2a and Figure 2c, and may cause an overfitting problem. On the other hand, the GT logit values of *PS* + Norm-softmax (D_1 and D_4) have lower confidence, represented with yellow to orange color. This is because synthetic classes generated near the original classes work as hard competitors (D_2 and D_3), which prevents excessively high confidence, while the confidence of main diagonals (D_1 and D_4) is still higher than that of competitors' diagonals (D_2 and D_3) with redder color for the same embedding. This smoothens the decision boundary, as depicted in Figure 2b and Figure 2d, and leads to stronger generalization.

Deformation	Norm-softmax	*PS* + Norm-softmax
Cutout	75.3	77.0 (+1.7)
Dropout	59.7	62.2 (+2.5)
Zoom in	64.3	65.6 (+1.3)
Zoom out	78.3	80.0 (+1.7)
Rotation	70.8	72.1 (+1.3)
Shearing	70.3	72.0 (+1.7)
Gaussian noise	65.1	67.2 (+2.1)
Gaussian blur	74.4	76.3 (+1.9)

Table 3: Recall@1(%) of input deformations with CARS196 trained models. Deformation details are presented in supplementary Section C.3.

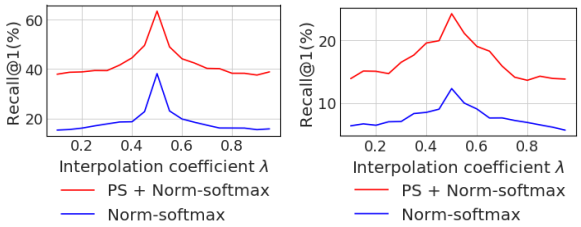

(a) Train set (b) Test set

Figure 5: Recall@1(%) of embedding deformations with trained networks on CARS196. For a gallery set, synthetic embeddings generated with λ and original embeddings are used. For a query set, synthetic embeddings are used to find other synthetic embeddings generated with same manner.

4.4 Robustness to Deformation

Input Deformation: To further evaluate the quality of representations learned with *Proxy Synthesis*, we perform a deformation test on the input data with trained networks. In Table 3, we evaluate the test data with several input deformations that are not used in training. A better-generalized model should be more robust to a large variety of input deformations. The result indicates that the network trained using *Proxy Synthesis* demonstrates significantly improved performance to input deformations.

Embedding Deformation: To see the robustness on embedding deformation of trained networks, we evaluate performance with synthetic embeddings. Figure 5 depicts a network trained with Norm-softmax loss struggling with low performance on both the train and test set. In contrast, a network trained with *Proxy Synthesis* performs almost twice as well when compared with Norm-softmax loss on both the train and test set. This demonstrates that *Proxy Synthesis* provides more robust embedding features, which also leads to robustness on *unseen* classes. Besides, the patterns of performance are similar to those discussed in Section 4.3. When λ is close to 0 and 1, the performance is low because of hard synthetics, and when λ is close to 0.5, the performance is

Loss	CUB200			CARS196			SOP		
	P@1	RP	MAP@R	P@1	RP	MAP@R	P@1	RP	MAP@R
Norm-softmax	65.65±0.30	35.99±0.15	25.25±0.13	83.16±0.25	36.20±0.26	26.00±0.30	75.67±0.17	50.01±0.22	47.13±0.22
PS+Norm-softmax	**69.19±0.34**	**37.32±0.29**	**26.40±0.29**	**85.70±0.24**	**38.33±0.31**	**28.31±0.32**	**76.73±0.15**	**51.46±0.21**	**48.52±0.20**
CosFace	67.32±0.32	37.49±0.21	26.70±0.23	85.52±0.24	37.32±0.28	27.57±0.30	75.79±0.14	49.77±0.19	46.92±0.19
PS+CosFace	**69.52±0.26**	**37.99±0.23**	**27.10±0.23**	**85.58±0.27**	**38.01±0.19**	**27.89±0.20**	**76.89±0.20**	**51.60±0.31**	**48.68±0.33**
ArcFace	67.50±0.25	37.31±0.21	26.45±0.20	85.44±0.28	37.02±0.29	27.22±0.30	76.20±0.27	50.27±0.38	47.41±0.40
PS+ArcFace	**68.79±0.31**	**37.46±0.26**	**26.79±0.27**	**85.59±0.25**	**38.31±0.22**	**28.24±0.20**	**77.21±0.20**	**51.90±0.23**	**49.02±0.21**
SoftTriple	67.73±0.39	37.34±0.19	26.51±0.20	84.49±0.26	37.03±0.21	28.07±0.21	76.12±0.17	50.21±0.18	47.35±0.19
PS+SoftTriple	**68.26±0.16**	**37.98±0.21**	**27.02±0.21**	**85.53±0.12**	**38.40±0.20**	**28.45±0.19**	**77.59±0.26**	**52.45±0.21**	**49.53±0.23**
Proxy-NCA	65.69±0.43	35.14±0.26	24.21±0.27	83.56±0.27	35.62±0.28	25.38±0.31	75.89±0.17	50.10±0.22	47.22±0.21
PS+Proxy-NCA	**66.02±0.29**	**35.73±0.24**	**24.84±0.22**	**84.61±0.19**	**36.39±0.25**	**26.04±0.27**	**76.78±0.21**	**51.39±0.27**	**48.44±0.27**
Proxy-anchor	69.73±0.31	38.23±0.37	27.44±0.35	86.20±0.21	39.08±0.31	29.37±0.29	75.37±0.15	50.19±0.14	47.25±0.15
PS+Proxy-anchor	**70.41±0.36**	**38.82±0.29**	**28.11±0.29**	**86.90±0.35**	**39.38±0.27**	**29.71±0.25**	**75.52±0.21**	**50.45±0.22**	**47.49±0.20**

Table 4: [MLRC evaluation] Performance (%) on the famous benchmarks of image retrieval task. We report the performance of concatenated 512-dim over 10 training runs. Bold numbers indicate the best score within the same loss and benchmark.

Regularizer	Softmax		Norm-softmax	
	CARS196	SOP	CARS196	SOP
Baseline	81.5	76.3	83.3	78
Virtual Softmax	77.3(-4.2)	76.2(-0.1)	-	-
Input Mixup	81.1(-0.4)	77.0(+0.7)	82.2(-1.1)	78.2(+0.2)
Manifold Mixup	81.6(+0.1)	77.5(+1.2)	83.6(+0.3)	78.4(+0.4)
Proxy Synthesis	**84.3(+2.8)**	**78.1(+1.8)**	**84.7(+1.4)**	**79.6(+1.6)**

Table 5: Recall@1(%) comparison with other regularizers in image retrieval task.

high because of relatively easy synthetics. Additional experiments are in the supplementary Section D.3.

4.5 Comparison with Other Regularizers

Further, we compare the proposed method with other regularizers, including Virtual Softmax, Input Mixup, and Manifold Mixup in the image retrieval task. Note that Virtual Softmax is not applicable to Norm-softmax loss because W_{virt} will always be constant 1. As presented in Table 5, Virtual Softmax degrades the performance of all cases with a margin of average -2.15%. Input Mixup degrades the performance on CARS196 with an average margin -0.75% and improves the performance on SOP with an average margin +0.45%. Manifold Mixup increases the performance of all cases with an average margin +0.5%. This illustrates that although these techniques are powerful for generalizing *seen* classes, such as classification tasks, they lack discriminative ability on *unseen* classes. On the other hand, *Proxy Synthesis* improves performance for all cases with a large margin of average +1.9% and achieves the best performance among all. Further analysis, including hyper-parameter search for Mixup and experiments in the classification task, is presented in the supplementary material Section D.4.

4.6 Comparison with State-of-the-Art

Finally, we compare the performance of our proposed method with state-of-the-art losses in two ways: *conventional* and *MLRC evaluation*. In *conventional evaluation*, the combinations of *Proxy Synthesis* with proxy-based losses improve performance by a large margin in every benchmark as presented in Table 6. For fine-grained datasets with few categories such as CUB200 and CARS196, the performance gain ranges between a minimum of +0.7% and a maximum of +2.8%, and the average improvement is +1.1%. For large-scale datasets with numerous categories such as SOP and In-Shop, the performance gain ranges between a minimum of +0.4% and a maximum of +1.4%, and the average improvement is +0.9%. Even in the specifically designed *MLRC evaluation*, Table 4 shows that *Proxy Synthesis* enhances performance for every metric and benchmark. Extended comparisons with Recall@k for *conventional evaluation* and performance of seperated 128-dim for *MLRC evaluation* are presented in the supplementary Section D.6.

Method	CUB200	CARS196	SOP	In-Shop
Softmax	64.2	81.5	76.3	90.4
PS+Softmax	**64.9(+0.7)**	**84.3(+2.8)**	**77.6(+1.3)**	**90.9(+0.5)**
Norm-softmax	64.9	83.3	78.6	90.4
PS+Norm-softmax	**66.0(+1.1)**	**84.7(+1.4)**	**79.6(+1.0)**	**91.5(+1.1)**
SphereFace	65.4	83.6	78.9	90.3
PS+SphereFace	**66.6(+1.2)**	**85.1(+1.5)**	**79.4(+0.5)**	**91.6(+1.3)**
CosFace	65.7	83.6	78.6	90.7
PS+CosFace	**66.6(+0.9)**	**84.6(+1.0)**	**79.3(+0.7)**	**91.4(+0.7)**
ArcFace	66.1	83.7	78.8	91.0
PS+ArcFace	**66.8(+0.7)**	**84.7(+1.0)**	**79.7(+0.9)**	**91.7(+0.7)**
Proxy-NCA	65.1	83.7	78.1	90.0
PS+Proxy-NCA	**66.4(+1.3)**	**84.5(+0.8)**	**79.1(+1.0)**	**91.4(+1.4)**
SoftTriple	65.4	84.5	78.3	91.1
PS+SoftTriple	**66.6(+1.2)**	**85.3(+0.8)**	**79.5(+1.2)**	**91.8(+0.7)**
Proxy-anchor†	68.4	86.1	79.1	91.5
PS+Proxy-anchor†	**69.2(+0.8)**	**86.9(+0.8)**	**79.8(+0.7)**	**91.9(+0.4)**

Table 6: [Conventional evaluation] Recall@1 (%) in image retrieval task. Bold numbers indicate the best score within the same loss and benchmark. † denotes exceptional settings as described in the supplementary Section C.2.

5 Conclusion

In this paper, we have proposed a novel regularizer called *Proxy Synthesis* for proxy-based losses that exploits synthetic classes for stronger generalization. Such effect is achieved by deriving class relations and smoothened decision boundaries. The proposed method provides a significant performance boost for all proxy-based losses and achieves state-of-the-art performance in image retrieval tasks.

References

Bartlett, P.; and Shawe-Taylor, J. 1999. Generalization performance of support vector machines and other pattern classifiers. *Advances in Kernel methods—support vector learning* 43–54.

Boudiaf, M.; Rony, J.; Ziko, I. M.; Granger, E.; Pedersoli, M.; Piantanida, P.; and Ayed, I. B. 2020. A unifying mutual information view of metric learning: cross-entropy vs. pairwise losses. *arXiv preprint arXiv:2003.08983* .

Chen, B.; Deng, W.; and Shen, H. 2018. Virtual class enhanced discriminative embedding learning. In *Advances in Neural Information Processing Systems*, 1942–1952.

Chopra, S.; Hadsell, R.; and LeCun, Y. 2005. Learning a similarity metric discriminatively, with application to face verification. In *2005 IEEE Computer Society Conference on Computer Vision and Pattern Recognition (CVPR'05)*, volume 1, 539–546. IEEE.

Deng, J.; Guo, J.; Xue, N.; and Zafeiriou, S. 2019. Arcface: Additive angular margin loss for deep face recognition. In *Proceedings of the IEEE Conference on Computer Vision and Pattern Recognition*, 4690–4699.

Duan, Y.; Zheng, W.; Lin, X.; Lu, J.; and Zhou, J. 2018. Deep adversarial metric learning. In *Proceedings of the IEEE Conference on Computer Vision and Pattern Recognition*, 2780–2789.

Fehervari, I.; Ravichandran, A.; and Appalaraju, S. 2019. Unbiased evaluation of deep metric learning algorithms. *arXiv preprint arXiv:1911.12528* .

Gordo, A.; Almazán, J.; Revaud, J.; and Larlus, D. 2016. Deep image retrieval: Learning global representations for image search. In *European conference on computer vision*, 241–257. Springer.

Gu, G.; and Ko, B. 2020. Symmetrical Synthesis for Deep Metric Learning. In *Proceedings of the AAAI Conference on Artificial Intelligence*.

Guo, H.; Mao, Y.; and Zhang, R. 2019. Mixup as locally linear out-of-manifold regularization. In *Proceedings of the AAAI Conference on Artificial Intelligence*, volume 33, 3714–3722.

Hermans, A.; Beyer, L.; and Leibe, B. 2017. In defense of the triplet loss for person re-identification. *arXiv preprint arXiv:1703.07737* .

Ioffe, S.; and Szegedy, C. 2015. Batch normalization: Accelerating deep network training by reducing internal covariate shift. *arXiv preprint arXiv:1502.03167* .

Kim, S.; Kim, D.; Cho, M.; and Kwak, S. 2020. Proxy Anchor Loss for Deep Metric Learning. *arXiv preprint arXiv:2003.13911* .

Ko, B.; and Gu, G. 2020. Embedding Expansion: Augmentation in Embedding Space for Deep Metric Learning. In *Proceedings of the IEEE Conference on Computer Vision and Pattern Recognition*.

Krause, J.; Stark, M.; Deng, J.; and Fei-Fei, L. 2013. 3d object representations for fine-grained categorization. In *Proceedings of the IEEE international conference on computer vision workshops*, 554–561.

Liu, W.; Wen, Y.; Yu, Z.; Li, M.; Raj, B.; and Song, L. 2017. Sphereface: Deep hypersphere embedding for face recognition. In *Proceedings of the IEEE conference on computer vision and pattern recognition*, 212–220.

Liu, Z.; Luo, P.; Qiu, S.; Wang, X.; and Tang, X. 2016. Deepfashion: Powering robust clothes recognition and retrieval with rich annotations. In *Proceedings of the IEEE conference on computer vision and pattern recognition*, 1096–1104.

Maaten, L. v. d.; and Hinton, G. 2008. Visualizing data using t-SNE. *Journal of machine learning research* 9(Nov): 2579–2605.

Mikolov, T.; Chen, K.; Corrado, G.; and Dean, J. 2013. Efficient estimation of word representations in vector space. *arXiv preprint arXiv:1301.3781* .

Movshovitz-Attias, Y.; Toshev, A.; Leung, T. K.; Ioffe, S.; and Singh, S. 2017. No fuss distance metric learning using proxies. In *Proceedings of the IEEE International Conference on Computer Vision*, 360–368.

Musgrave, K.; Belongie, S.; and Lim, S.-N. 2020. A Metric Learning Reality Check. *arXiv preprint arXiv:2003.08505* .

Oh Song, H.; Xiang, Y.; Jegelka, S.; and Savarese, S. 2016. Deep metric learning via lifted structured feature embedding. In *Proceedings of the IEEE conference on computer vision and pattern recognition*, 4004–4012.

Pereyra, G.; Tucker, G.; Chorowski, J.; Kaiser, Ł.; and Hinton, G. 2017. Regularizing neural networks by penalizing confident output distributions. *arXiv preprint arXiv:1701.06548* .

Qian, Q.; Shang, L.; Sun, B.; Hu, J.; Li, H.; and Jin, R. 2019. SoftTriple Loss: Deep Metric Learning Without Triplet Sampling. In *Proceedings of the IEEE International Conference on Computer Vision*, 6450–6458.

Sohn, K. 2016. Improved deep metric learning with multi-class n-pair loss objective. In *Advances in neural information processing systems*, 1857–1865.

Verma, V.; Lamb, A.; Beckham, C.; Najafi, A.; Mitliagkas, I.; Courville, A.; Lopez-Paz, D.; and Bengio, Y. 2018. Manifold mixup: Better representations by interpolating hidden states. *arXiv preprint arXiv:1806.05236* .

Wah, C.; Branson, S.; Welinder, P.; Perona, P.; and Belongie, S. 2011. The caltech-ucsd birds-200-2011 dataset .

Wang, F.; Cheng, J.; Liu, W.; and Liu, H. 2018a. Additive margin softmax for face verification. *IEEE Signal Processing Letters* 25(7): 926–930.

Wang, F.; Xiang, X.; Cheng, J.; and Yuille, A. L. 2017. Normface: L2 hypersphere embedding for face verification. In *Proceedings of the 25th ACM international conference on Multimedia*, 1041–1049.

Wang, H.; Wang, Y.; Zhou, Z.; Ji, X.; Gong, D.; Zhou, J.; Li, Z.; and Liu, W. 2018b. Cosface: Large margin cosine loss for deep face recognition. In *Proceedings of the IEEE Conference on Computer Vision and Pattern Recognition*, 5265–5274.

Weinberger, K. Q.; and Saul, L. K. 2009. Distance metric learning for large margin nearest neighbor classification. *Journal of Machine Learning Research* 10(Feb): 207–244.

Wen, Y.; Zhang, K.; Li, Z.; and Qiao, Y. 2016. A discriminative feature learning approach for deep face recognition. In *European conference on computer vision*, 499–515. Springer.

Yu, R.; Dou, Z.; Bai, S.; Zhang, Z.; Xu, Y.; and Bai, X. 2018. Hard-aware point-to-set deep metric for person reidentification. In *Proceedings of the European Conference on Computer Vision (ECCV)*, 188–204.

Zhai, A.; and Wu, H.-Y. 2018. Classification is a Strong Baseline for Deep Metric Learning. *arXiv preprint arXiv:1811.12649* .

Zhang, H.; Cisse, M.; Dauphin, Y. N.; and Lopez-Paz, D. 2017. mixup: Beyond empirical risk minimization. *arXiv preprint arXiv:1710.09412* .

Zhang, Z.; and Saligrama, V. 2016. Zero-shot learning via joint latent similarity embedding. In *proceedings of the IEEE Conference on Computer Vision and Pattern Recognition*, 6034–6042.

Zhao, Y.; Jin, Z.; Qi, G.-j.; Lu, H.; and Hua, X.-s. 2018. An adversarial approach to hard triplet generation. In *Proceedings of the European conference on computer vision (ECCV)*, 501–517.

Zheng, W.; Chen, Z.; Lu, J.; and Zhou, J. 2019. Hardness-aware deep metric learning. In *Proceedings of the IEEE Conference on Computer Vision and Pattern Recognition*, 72–81.